Determination of the Local Environment of the Metals in $[Cr^{III}_2Co^{II}O(MeCO_2)_6(py)_3]\cdot py$ (py = pyridine) by Chromium and Cobalt K-edge Extended X-Ray Absorption Fine Structure. Geometric and Charge-polarisation Influences on Cr–O–Cr Superexchange‡

A. Bryan Edwards,[a] John M. Charnock,[a] C. David Garner*,[a] and Antony B. Blake*,†,[b]

[a] *Department of Chemistry, University of Manchester, Manchester M13 9PL, UK*

[b] *School of Chemistry, University of Hull, Hull HU6 7RX, UK*

X-Ray absorption spectra at the chromium and cobalt K edges have been recorded for the metal-disordered compound $[Cr^{III}_2Co^{II}O(MeCO_2)_6(py)_3]\cdot py$ (py = pyridine) and the associated extended X-ray absorption fine structure (EXAFS) analysed using curved-wave theory with the inclusion of multiple scattering for the co-ordinated pyridine and acetate groups; a corresponding study for the iron K-edge EXAFS of $[Fe_3O(MeCO_2)_6(py)_3]\cdot py$ was accomplished as a calibrant of the interpretive procedure. The dimensions Cr–μ_3-O 1.87, Co–μ_3-O 1.95, Cr–O (acetate) 1.98, Co–O (acetate) 2.09, Cr–N 2.26, Co–N 2.24, Cr···Cr 3.30 and Cr···Co 3.28 Å were obtained from the analysis of the EXAFS, with good agreement between the values of the Cr···Co distance obtained independently from the analyses of the chromium and cobalt EXAFS. The metal–ligand and –metal distances are in good agreement with crystallographic data on related compounds. The difference in the Cr–μ_3-O and Co–μ_3-O distances indicates that the central (μ_3) oxygen atom is slightly displaced (*ca.* 0.05 Å) from the centre of the metal triangle, away from the Co^{II} and towards the point midway between the two chromium(III) atoms. Such a structural change and the increased electron density of the central oxygen combine to produce a marked increase in the Cr^{III}–O–Cr^{III} superexchange and a reduced ligand field at the chromium(III) sites, for the Cr_2CoO system as compared with Cr^{III}_3O analogues.

In a study of the magnetic properties of the mixed-metal complexes $[Cr^{III}_2M^{II}O(MeCO_2)_6(py)_3]\cdot py$ and $[Fe^{III}_2M^{II}O(MeCO_2)_6(py)_3]\cdot py$ (M = Mg, Mn, Co or Ni; py = pyridine) the remarkable observation was made that the strength of the M^{III}–M^{III} spin–spin exchange interaction (J_{12}) is significantly *increased* over its value in the corresponding Cr^{III}_3 or Fe^{III}_3 complex.[1] The increase is by a factor of *ca.* 2.3, and this factor varies relatively little with the nature of M^{II} (Cr_2Ni, 2.35; Cr_2Co, 2.4; Fe_2Mg, 2.1; Fe_2Mn, 2.1; Fe_2Ni, 2.4 cm^{-1}). In the case of the chromium compounds the *increase* in J_{12} is accompanied by a 6% *decrease* in the average ligand-field strength at the chromium(III) site, as determined by electronic absorption spectroscopy.

In view of the steric constraints on the geometry of the M_3O unit imposed by the acetate cage, the reason for this pronounced increase in J_{12}, as a result of replacing the third Cr^{III} by a divalent ion, is not immediately obvious. One possibility is that the larger metal(II) ion causes a physical displacement of the central O atom (which is believed to constitute the main superexchange pathway), giving a shorter M^{III}–O bond and a larger M^{III}–O–M^{III} angle, both of which should increase the strength of antiferromagnetic coupling.[2] However, the observed reduction in ligand-field strength certainly does not suggest a shorter M^{III}–O bond. Moreover, if geometric factors are the primary cause, replacing Ni^{II} (radius[3] 0.69 Å) by Mn^{II} (0.83 Å) might have been expected to change J_{12} at least as much as replacing Fe^{III} (0.645 Å) by Ni^{II}, contrary to experimental observation.[1] The suggestion was therefore made that the effect of M^{II} on J_{12} might be due mainly to *polarisation of the in-plane p orbitals of the* μ_3-O *atom*, arising from an asymmetric charge distribution in the M_3 triangle.[1]

Whether the M_3O moiety in $[M_3O(MeCO_2)_6(py)_3]\cdot py$ is significantly distorted from the three-fold symmetry usually observed cannot be determined by X-ray diffraction for the mixed-metal systems because of the disorder of the metals over the three sites. Thus, the $Cr^{III}_2M^{II}$ and $Fe^{III}_2M^{II}$ compounds with M^{II} = Mn^{II} or Co^{II} crystallise, like their mixed-valence $Mn^{III}_2Mn^{II}$ and $Fe^{III}_2Fe^{II}$ analogues, in a trigonal space group, with the divalent ion randomly occupying one of the three equivalent metal sites.[1,4,5] The compounds containing Mg^{II} and Ni^{II} crystallise in the monoclinic system with no crystallographically imposed symmetry, but the crystal structures of the $Cr^{III}_2Mg^{II}$ and $Cr^{III}_2Ni^{II}$ compounds indicate that the divalent ion locations in these compounds are also largely, if not completely, disordered.[6] Similarly, the Co^{II} is randomly distributed over the three metal sites of $[Mn_2CoO(MeCO_2)_6(py)_3]\cdot MeCO_2H$.[7]

Extended X-ray absorption fine structure (EXAFS) is an element-specific structural technique that does not depend on the presence of long-range order, and it has been widely used to determine metal-atom environments in biomolecules and other non-crystalline or disordered materials.[8] Therefore, we have recorded and analysed the EXAFS of $[Cr_2CoO(MeCO_2)_6(py)_3]\cdot py$ at both the chromium and cobalt K edges so as to circumvent the disorder problem and to determine independently the local environments of the Cr and Co atoms. In this way we hoped to establish whether M^{III}–O bond length or M–O–M angle differences were sufficiently large to account for the observed increase in J_{12}. A point of added interest was to see the level of consistency within the structural details of the Cr_2CoO system, as derived from the independent chromium and cobalt K-edge EXAFS data sets.

† *Present address:* PO Box 89A, Kangaroo Valley, New South Wales 2577, Australia.

‡ *Non-SI unit employed:* eV ≈ 1.60 × 10^{-19} J.

Experimental

The complexes $[Fe_3O(MeCO_2)_6(py)_3]\cdot py$ and $[Cr_2CoO(MeCO_2)_6(py)_3]\cdot py$ were prepared as described previously.[1] Each sample was ground into a fine powder and evenly diluted with boron nitride then placed in an aluminium sample holder and held in place with Sellotape. X-Ray absorption spectra were recorded at each of the metal K edge(s), from *ca.* 300 eV before to *ca.* 1000 eV beyond the edge, for each sample at room temperature. Data were collected in transmission mode on Station 7.1 at the Daresbury Laboratory Synchrotron Radiation Source (SRS) with beam energy 2 GeV and beam current of 170 mA, using a Si(111) order-sorting, double-crystal, monochromator set to 50% transmission. A single scan was recorded for each spectrum, increasing the count time per point from 1 s at the start of the EXAFS region to 8 s at the end, at k increments of 0.04 $Å^{-1}$.

Calibration and background subtraction of the raw data was performed by use of the Daresbury Laboratory programs EXCALIB and EXBACK, respectively. The isolated EXAFS data were analysed using EXCURV 92,[9] employing the spherical wave approximation, including multiple-scattering contributions from the pyridine rings and the acetate ligands.[10–12] Phase shifts were derived from *ab initio* calculations using Hedin–Lundqvist potentials and von Bart ground states.[13]

Results and Discussion

EXAFS Interpretation.—The Fe K-edge EXAFS of the valence-delocalised compound $[Fe^{III}_2Fe^{II}O(MeCO_2)_6(py)_3]\cdot py$ (Fig. 1) was interpreted as a calibrant of the interpretive procedure. Back scattering was observed from shells of up to 5 Å from the Fe (Fig. 2 and Table 1). The interatomic distances were initially set at the crystallographic values[5] and each distance from iron, together with its associated Debye–Waller parameter (which includes both thermal and static disorder), and E_f were refined keeping the co-ordination numbers constant. For the inner co-ordination shell the four acetate oxygens were refined as a single shell, with the μ_3-O and N_{py} atoms treated as separate shells. The back scattering from other O and C atoms of the co-ordinated acetates and the other atoms of the pyridine ring was treated using multiple scattering and restrained refinement for the atoms of the acetate and pyridine groups.[10–12] The agreement between the distances obtained from the analysis of the iron K-edge EXAFS of $[Fe_3O(MeCO_2)_6(py)_3]\cdot py$ and X-ray crystallography[5] (Table 1) is within ±0.03 Å for the inner co-ordination shell. This level of agreement was obtained for the outer shells with the notable exception of the Fe···Fe separation (EXAFS 3.25 Å, X-ray crystallography 3.307 Å) and it is noted that the back scattering from the iron shell involves some interference with the carbon shell of the acetate (3.031 Å) and pyridine (3.135 Å) ligands. However, the inclusion of the iron shell is statistically significant.[15]

The approach outlined above for $[Fe_3O(MeCO_2)_6(py)_3]\cdot py$ was employed to simulate the chromium and cobalt K-edge EXAFS for $[Cr_2CoO(MeCO_2)_6(py)_3]\cdot py$. For the cobalt EXAFS the chromium back scattering was assumed to arise from a single shell of atoms but for the chromium EXAFS the back-scattered contributions of Cr and Co were treated using separate, singly occupied shells. The results of these simulations of the experimental data are illustrated in Figs. 3 and 4 and summarised in Table 2.

The metal–ligand bond distances obtained from the analysis of the chromium and cobalt K-edge EXAFS of $[Cr_2CoO(MeCO_2)_6(py)_3]\cdot py$ are in the normal range[16] for chromium(III) and cobalt(II) complexes, with each Co^{II}–O distance longer than the corresponding Cr^{III}–O but both systems have similar M–N distances. The average $M–O_{acetate}$ distance in $[Cr_2CoO(MeCO_2)_6(py)_3]\cdot py$ of 2.02 Å is similar to that (2.00 Å) in the corresponding Cr_2Ni system.[6] The average $M–N_{py}$ distance in $[Cr_2CoO(MeCO_2)_6(py)_3]\cdot py$ of 2.25 Å is 0.1 Å longer than in the Cr_2Ni system but similar to that in the Cr_2Mg compound.[6] The Co^{II}–μ_3-O and Cr^{III}–μ_3-O distances of 1.95 and 1.87 Å, respectively, suggest a small, *ca.* 0.05 Å, displacement

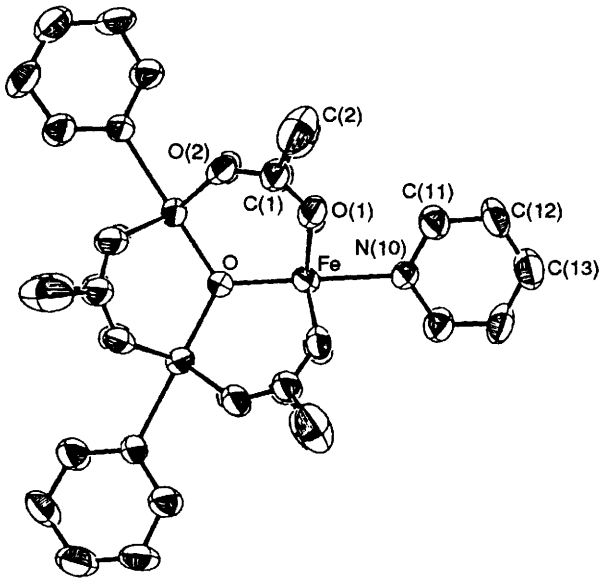

Fig. 1 An ORTEP[14] plot of the molecular structure of $[Fe_3O(MeCO_2)_6(py)_3]\cdot py$. Atoms are shown as 50% equiprobability ellipsoids. Reproduced from ref. 5 with permission

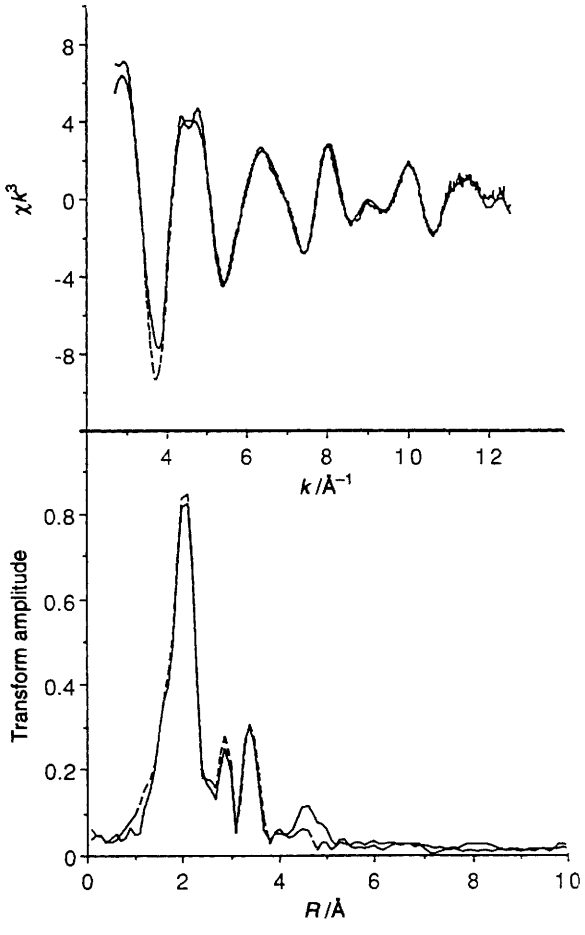

Fig. 2 Iron K-edge EXAFS × k^3 of $[Fe_3O(MeCO_2)_6(py)_3]\cdot py$ recorded at room temperature (——) and a simulation based on the parameters listed in Table 1 (– – –) together with their Fourier transforms

Table 1 Parameters[a] obtained from the analysis of the iron K-edge EXAFS of $[Fe_3O(MeCO_2)_6(py)_3]\cdot py$ and shell distances obtained by X-ray crystallography[5]

		EXAFS		Crystal structure		
Shell	Occupation number[b]	R/Å	$2\sigma^2$/Å^2	R/Å	Range/Å	Assignment
O	1	1.88	0.014	1.909	—	Fe–μ_3-O
O	4	2.05	0.014	2.071	2.064–2.077	Fe–OCO$_{ac}$
N	1	2.23	0.024	2.215	—	Fe–N$_{py}$
C	4	3.00	0.015	3.031[c]	3.007–3.055	Fe–OCO$_{ac}$
C	2	3.14	0.039	3.135[c]	—	Fe–C$^2_{py}$
Fe	2	3.25	0.021	3.307	—	Fe···Fe
O	4	3.38	0.078	3.413[c]	3.382–3.443	Fe–OCO_{ac}
C	4	4.36	0.032	4.381[c]	4.364–4.398	Fe–CH$_{3ac}$
C	2	4.44	0.061	4.428[c]	4.416–4.440	Fe–C$^3_{py}$
C	1	4.96	0.054	4.960[c]	—	Fe–C$^4_{py}$

[a] R = Shell distance, σ = Debye–Waller parameter. [b] Maintained at the crystallographic value. [c] Position constrained by restrained refinement.[12]

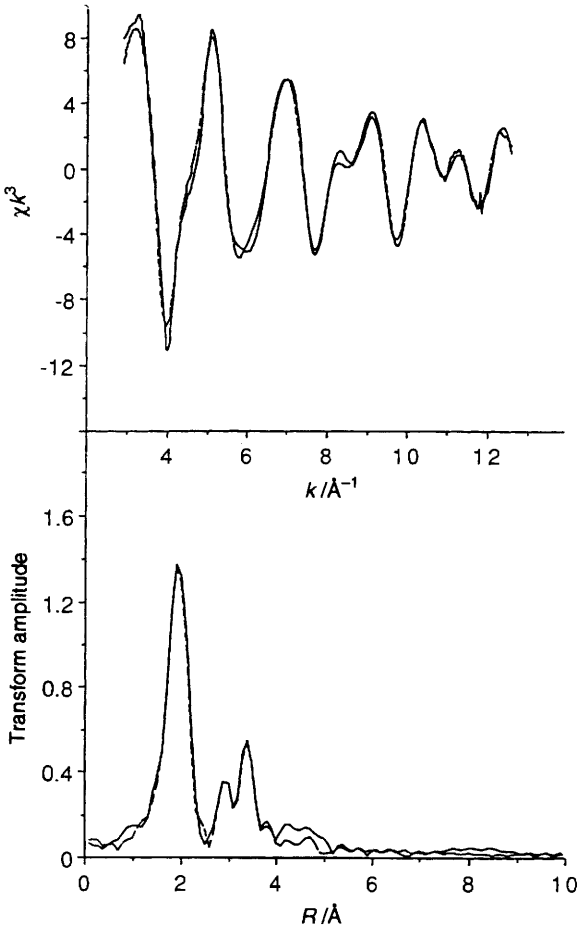

Fig. 3 Chromium K-edge EXAFS × k^3 of $[Cr_2CoO(MeCO_2)_6(py)_3]\cdot py$ recorded at room temperature (——) and a simulation based on the parameters listed in Table 2 (– – –) together with their Fourier transforms

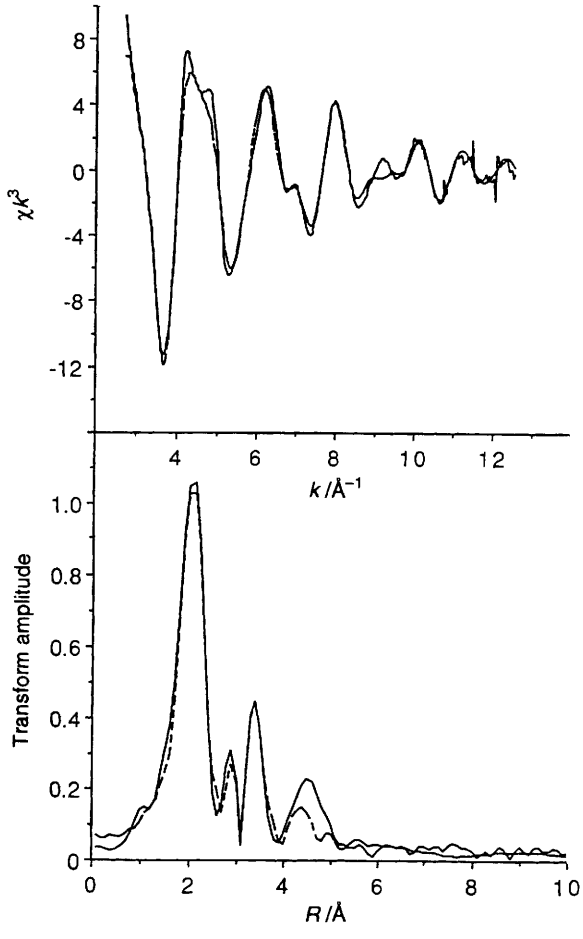

Fig. 4 Cobalt K-edge EXAFS × k^3 of $[Cr_2CoO(MeCO_2)_6(py)_3]\cdot py$ recorded at room temperature (——) and a simulation based on the parameters listed in Table 2 (– – –) together with their Fourier transforms

of the central oxygen away from the Co^{II} and towards the point midway between the chromium(III) atoms; this displacement is less than that (0.14 Å) in the valence-localised compound $[Mn^{III}_2Mn^{II}O(MeCO_2)_6(3\text{-}ClC_5H_4N)_3]$.[17] The average of the Cr–μ_3-O and Co–μ_3-O distances, 1.90 Å, matches those in the Cr_2Mg and Cr_2Ni systems [of 1.897(8) and 1.895(12) Å, respectively].[6] The metal–metal separations, determined independently from the chromium and cobalt K-edge EXAFS simulations, are (Table 2) not significantly different and average as 3.29 Å. The Cr–μ_3-O–Cr and Cr–μ_3-O–Co bond angles follow from the Co^{II}–μ_3-O, Cr^{III}–μ_3-O and the metal–metal separations and are estimated as 123.9 and 118.3°, respectively. Thus, as expected,[6] the Cr_2CoO unit is essentially planar.

Relation of Structure to Magnetic Behaviour.—Table 3 gives structural data and J_{12} values for some bi- and tri-nuclear chromium complexes, in which two chromium(III) ions are linked by an oxygen atom and two bridging carboxylate groups, arranged according to the nature of the third group attached to the bridging O atom. In the cases considered[18–26] in Table 3 the Cr^{III}–O bond lengths and Cr^{III}–O–Cr^{III} angles all lie

Table 2 Parameters[a] obtained from the analysis of the chromium and cobalt K-edge EXAFS of $[Cr_2CoO(MeCO_2)_6(py)_3]\cdot py$

Shell	Occupation number[b]	R/Å	$2\sigma^2$/Å^2	Assignment
Chromium K edge				
O	1	1.87	0.002	Cr–μ_3-O
O	4	1.98	0.005	Cr–*O*CO$_{ac}$
N	1	2.26	0.007	Cr–N$_{py}$
C	4	2.95[c]	0.008	Cr–O*C*O$_{ac}$
C	2	2.99[c]	0.007	Cr–C$^2_{py}$
O	4	3.12[c]	0.015	Cr–OC*O*$_{ac}$
Co	1	3.28	0.008	Cr · · · Co
Cr	1	3.30	0.012	Cr · · · Cr
C	4	4.27[c]	0.012	Cr–*C*H$_{3ac}$
C	2	4.40[c]	0.009	Cr–C$^3_{py}$
C	1	4.98[c]	0.010	Cr–C$^4_{py}$
Cobalt K edge				
O	1	1.95	0.002	Co–μ_3-O
O	4	2.09	0.007	Co–*O*CO$_{ac}$
N	1	2.24	0.004	Co–N$_{py}$
C	4	2.94[c]	0.007	Co–O*C*O$_{ac}$
C	2	3.05[c]	0.005	Co–C$^2_{py}$
O	4	3.13[c]	0.020	Co–OC*O*$_{ac}$
Cr	2	3.28	0.018	Co · · · Cr
C	4	4.32[c]	0.012	Co–*C*H$_{3ac}$
C	2	4.45[c]	0.010	Co–C$^3_{py}$
C	1	5.00[c]	0.012	Co–C$^4_{py}$

[a] R = Shell distance, σ = Debye–Waller parameter. [b] Fixed at value expected for the structure. [c] Position constrained by restrained refinement.[12]

Table 3 The Cr^{III}–O–Cr^{III} dimensions and exchange parameters in selected complexes involving carboxylate bridges

Exchange cluster	Cr^{III}–O/Å	Cr^{III}–O–Cr^{III}/°	$-J_{12}$/cm^{-1}	Ref.
Cr_2O–Cr^{III}	1.90	120	10.7 ± 1.5	*a*
Cr_2O–Fe^{III}	1.89	120	10	*b*
Cr_2O–H	1.92	123	11.2 ± 0.2	*c*
Cr_2O–Co^{II}	1.87	124	27 ± 2	*d*
Cr_2O–Ni^{II}			26 ± 1	*e*
Cr_2O	1.85	121	28 ± 1	*f*

[a] $[Cr_3O(MeCO_2)_6(H_2O)_3]Cl\cdot 6H_2O$;[18,19] $[Cr_3O(MeCO_2)_6(H_2O)_3]Cl\cdot 3SC(NH_2)_2\cdot 2H_2O$;[20] $[Cr_3O(na)_6(H_2O)_3][ClO_4]_7$ (Hna = nicotinic acid).[21] Note that $Cr^{III}{}_3O$ complexes usually appear to have two slightly different J_{12} values,[22] but the difference is only *ca.* 10–20% and the average value does not vary greatly. [b] $[Cr_2FeO(CH_2ClCO_2)_6(H_2O)_3][NO_3]$.[23,24] [c] $[Cr_2(OH)(HCO_2)_2(H_2O)_6][O_3SC_6M_4Me\text{-}p]_3$.[25] [d] $[Cr_2CoO(MeCO_2)_6(py)_3]$, this work and ref. 1; J_{12} here is a parameter in a fairly complex theoretical model,[1] but its value appears to be reasonably well determined by the data. [e] $[Cr_2NiO(MeCO_2)_6(py)_3]$.[1] The dimensions are assumed to be similar to those in the Cr_2Co compound. [f] $[Cr_2O(MeCO_2)_2L_3][BPh_4]_2$ (L = 1,4,7-trimethyl-1,4,7-triazacyclononane).[26]

within fairly narrow ranges. The values of J_{12}, however, fall into two distinct groups: around -11 cm^{-1} when the third group attached to the O atom is Cr^{III}, Fe^{III} or H^+, and around -27 cm^{-1} when it is Co^{II}, Ni^{II}, or is absent.

The results of the EXAFS studies of $[Cr_2CoO(MeCO_2)_6(py)_3]\cdot py$ are consistent with a small (*ca.* 0.05 Å) displacement of the μ_3-O atom away from Co^{II} towards the point midway between the chromium(III) atoms, and an increase in the Cr^{III}–O–Cr^{III} angle to *ca.* 124°. These perturbations of a regular M_3O triangle are in the direction that is generally associated with increased exchange coupling in chromium(III) complexes.[2] On their own we believe they are insufficient to explain the increase in $-J_{12}$ by a factor of *ca.* 2.4, on replacing Cr^{III} attached to a Cr^{III}–O–Cr^{III} centre by Co^{II}. As noted above, this substitution also reduces the average ligand field at the chromium(III) centres.[1] A possible explanation is that the displacement of the μ_3-O atom towards the region between the two chromium(III) atoms coupled with the polarisation of the oxygen's in-plane p orbital in the same direction, due to the lower charge of Co^{II} as compared with Cr^{III}, increases the overlap between the oxygen in-plane p and the chromium in-plane d_π orbitals, thereby raising the energy of the corresponding antibonding molecular orbitals and decreasing the ligand-field splitting. Since there is evidence that these orbital overlaps provide the most effective superexchange pathway,[1] and theoretical arguments suggest that the antiferromagnetic exchange should increase with increasing overlap[27] and with increasing electron density on the bridging group,[28] this would also be expected to lead to an increase in $-J_{12}$, as is observed. Thus, the apparently inconsistent magnetic and spectroscopic observations are reconciled.

The same arguments could be put forward to account for the ratio of the J_{12} parameter of the $M^{III}{}_2O$–M^{II} system to that of the corresponding $M^{III}{}_2O$–M^{III} system for the other compounds in Table 3. In principle, they could also be used to explain the similar ratio observed between the exchange parameter of $Cr^{III}{}_2O$ and that of $Cr^{III}{}_2O$–H, taking into account polarisation of the oxygen in-plane p orbitals by the charge of the proton. However, in this case a large part of the decrease in the magnitude of J_{12} could reasonably be attributed to the more substantial (0.07 Å) increase in the Cr^{III}–O bond length on protonation. More surprising is the fact that the actual J_{12} value of $Cr^{III}{}_2O$–H is similar to that of $Cr^{III}{}_2O$–Cr^{III}, and that of $Cr^{III}{}_2O$ to that of $Cr^{III}{}_2O$–M^{II}. The coincidental balancing of several factors may be involved here.

Acknowledgements

We thank the SERC for the provision of a studentship (to A. B. E.) and the Director of the Daresbury Laboratory for the provision of facilities.

References

1 A. B. Blake, A. Yavari, W. E. Hatfield, and C. N. Sethulekshmi, *J. Chem. Soc., Dalton Trans.*, 1985, 2509.
2 R. P. Scaringe, D. J. Hodgson and W. E. Hatfield, *Transition Met. Chem.*, 1981, **6**, 340; W. E. Hatfield, J. J. MacDougall and R. E. Shepherd, *Inorg. Chem.*, 1981, **20**, 4216; D. J. Hodgson, in *Magneto-Structural Correlations in Exchange Coupled Systems*, eds. R. D. Willett, D. Gatteschi and O. Kahn, D. Reidel, Dordrecht, 1985, pp. 497–522.
3 R. D. Shannon, *Acta Crystallogr., Sect. A*, 1976, **32**, 751.
4 A. R. E. Baikie, M. B. Hursthouse, D. B. New and P. Thornton, *J. Chem. Soc., Chem. Commun.*, 1978, 62; J. B. Vincent, H.-R. Chang, K. Folting, J. C. Huffman, G. Christou and D. N. Hendrickson, *J. Am. Chem. Soc.*, 1987, **109**, 5703.
5 S. E. Woehler, R. J. Wittebort, S. M. Oh, T. Kambara, D. N. Hendrickson, D. Inniss and C. E. Strouse, *J. Am. Chem. Soc.*, 1987, **109**, 1063.
6 A. B. Blake, M. B. Hursthouse, M. Motevalli and R. L. Short, unpublished work.
7 R. D. Cannon, U. A. Jayasooriya, L. Montri, A. K. Saad, E. Karu, S. K. Bollen, W. R. Sanderson, A. K. Powell and A. B. Blake, *J. Chem. Soc., Dalton Trans.*, 1993, 2005.
8 C. D. Garner, *Adv. Inorg. Chem.*, 1991, **36**, 303 and refs. therein; D. C. Koningsberger and R. Prins (Editors), *X-Ray Absorption: Principles, Applications, Techniques of EXAFS, SEXAFS and XANES*, Wiley, New York, 1988; A. B. Blake, J. R. Chipperfield, S. Lau and D. E. Webster, *J. Chem. Soc., Dalton Trans.*, 1990, 3719.
9 N. Binsted, J. W. Campbell, S. J. Gurman and P. C. Stephenson, EXCURV 92 program, SERC Daresbury Laboratory, 1991.
10 P. A. Lee and J. B. Pendry, *Phys. Rev. B*, 1975, **11**, 2795.
11 S. J. Gurman, N. Binsted and I. Ross, *J. Phys. C*, 1984, **17**, 143; 1986, **19**, 1845.
12 N. Binsted, R. W. Strange and S. S. Hasnain, *Biochemistry*, 1992, **31**, 12117.
13 L. Hedin and S. Lundqvist, *Solid State Phys.*, 1969, **23**, 1.

14 C. K. Johnson, ORTEP, Report ORNL-5138, Oak Ridge National Laboratory, Oak Ridge, TN, 1976.
15 R. W. Joyner, K. J. Martin and P. Meehan, *J. Phys. C*, 1987, **20**, 4005.
16 A. G. Orpen, L. Brammer, F. H. Allen, O. Kennard, D. G. Watson and R. Taylor, *J. Chem. Soc., Dalton Trans.*, 1989, S1.
17 A. R. E. Baikie, M. B. Hursthouse, L. New, P. Thornton and R. G. White, *J. Chem. Soc., Chem. Commun.*, 1980, 684.
18 S. C. Chang and G. A. Jeffrey, *Acta Crystallogr., Sect. B*, 1970, **26**, 673.
19 A. Earnshaw, B. N. Figgis and J. Lewis, *J. Chem. Soc. A*, 1966, 1656; M. Sorai, M. Takichi, H. Suga and S. Seki, *J. Phys. Soc. Jpn.*, 1971, **30**, 750; J. Ferguson and H. U. Güdel, *Chem. Phys. Lett.*, 1972, **17**, 547.
20 E. Karu, C. E. Anson, R. D. Cannon, U. A. Jayasooriya and A. K. Powell, *Acta Crystallogr., Sect. C*, 1993, **49**, 1929.
21 E. Gonzalez-Vergara, J. Hegenauer, P. Saltman, M. Sabat and J. A. Ibers, *Inorg. Chim. Acta*, 1982, **66**, 115.
22 R. D. Cannon and R. P. White, *Prog. Inorg. Chem.*, 1988, **36**, 195.
23 Y. V. Rakitin, T. A. Zhemchuzhnikova and V. V. Zelentsov, *Inorg. Chim. Acta*, 1977, **23**, 145.
24 T. Glowiak, M. Kubiak, T. Szymanska-Buzar and B. Jezowska-Trzebiatowska, *Acta Crystallogr., Sect. B*, 1977, **33**, 3106.
25 P. N. Turowski, A. Bino and S. J. Lippard, *Angew. Chem., Int. Ed. Engl.*, 1990, **29**, 811.
26 L. L. Martin, K. Wieghardt, G. Blondin, J.-J. Girerd, B. Nuber and J. Weiss, *J. Chem. Soc., Chem. Commun.*, 1990, 1767.
27 O. Kahn and M. F. Charlot, *Nouv. J. Chim.*, 1980, **4**, 567.
28 P. J. Hay, J. C. Thibeault and R. Hoffmann, *J. Am. Chem. Soc.*, 1975, **97**, 4884.

Received 3*rd March* 1995; *Paper* 5/01302J